

**OFFICE OF CIVILIAN RADIOACTIVE WASTE MANAGEMENT  
ANALYSIS/MODEL COVER SHEET**

1. QA: QA

Page: 1 of: 32

**Complete Only Applicable Items**

<p>2. <input checked="" type="checkbox"/> <b>Analysis</b>      Check all that apply</p> <table border="1" style="width:100%; border-collapse: collapse;"> <tr> <td style="width:20%;">Type of Analysis</td> <td> <input type="checkbox"/> Engineering  <input type="checkbox"/> Performance Assessment  <input checked="" type="checkbox"/> Scientific                 </td> </tr> <tr> <td>Intended Use of Analysis</td> <td> <input type="checkbox"/> Input to Calculation  <input checked="" type="checkbox"/> Input to another Analysis or Model  <input checked="" type="checkbox"/> Input to Technical Document  <input checked="" type="checkbox"/> Input to other Technical Products                 </td> </tr> <tr> <td colspan="2">Describe use: To be used as input to WPD PMR and SRCR</td> </tr> </table>	Type of Analysis	<input type="checkbox"/> Engineering <input type="checkbox"/> Performance Assessment <input checked="" type="checkbox"/> Scientific	Intended Use of Analysis	<input type="checkbox"/> Input to Calculation <input checked="" type="checkbox"/> Input to another Analysis or Model <input checked="" type="checkbox"/> Input to Technical Document <input checked="" type="checkbox"/> Input to other Technical Products	Describe use: To be used as input to WPD PMR and SRCR		<p>3. <input checked="" type="checkbox"/> <b>Model</b>      Check all that apply</p> <table border="1" style="width:100%; border-collapse: collapse;"> <tr> <td style="width:20%;">Type of Model</td> <td> <input type="checkbox"/> Conceptual Model      <input type="checkbox"/> Abstraction Model  <input checked="" type="checkbox"/> Mathematical Model      <input type="checkbox"/> System Model  <input checked="" type="checkbox"/> Process Model                 </td> </tr> <tr> <td>Intended Use of Model</td> <td> <input type="checkbox"/> Input to Calculation  <input checked="" type="checkbox"/> Input to another Model or Analysis  <input checked="" type="checkbox"/> Input to Technical Document  <input checked="" type="checkbox"/> Input to other Technical Products                 </td> </tr> <tr> <td colspan="2">Describe use: To be used as input to WPD PMR and SRCR</td> </tr> </table>	Type of Model	<input type="checkbox"/> Conceptual Model <input type="checkbox"/> Abstraction Model <input checked="" type="checkbox"/> Mathematical Model <input type="checkbox"/> System Model <input checked="" type="checkbox"/> Process Model	Intended Use of Model	<input type="checkbox"/> Input to Calculation <input checked="" type="checkbox"/> Input to another Model or Analysis <input checked="" type="checkbox"/> Input to Technical Document <input checked="" type="checkbox"/> Input to other Technical Products	Describe use: To be used as input to WPD PMR and SRCR	
Type of Analysis	<input type="checkbox"/> Engineering <input type="checkbox"/> Performance Assessment <input checked="" type="checkbox"/> Scientific												
Intended Use of Analysis	<input type="checkbox"/> Input to Calculation <input checked="" type="checkbox"/> Input to another Analysis or Model <input checked="" type="checkbox"/> Input to Technical Document <input checked="" type="checkbox"/> Input to other Technical Products												
Describe use: To be used as input to WPD PMR and SRCR													
Type of Model	<input type="checkbox"/> Conceptual Model <input type="checkbox"/> Abstraction Model <input checked="" type="checkbox"/> Mathematical Model <input type="checkbox"/> System Model <input checked="" type="checkbox"/> Process Model												
Intended Use of Model	<input type="checkbox"/> Input to Calculation <input checked="" type="checkbox"/> Input to another Model or Analysis <input checked="" type="checkbox"/> Input to Technical Document <input checked="" type="checkbox"/> Input to other Technical Products												
Describe use: To be used as input to WPD PMR and SRCR													

4. Title:  
Hydrogen Induced Cracking of Drip Shield

5. Document Identifier (including Rev. No. and Change No., if applicable):  
ANL-EBS-MD-000006 REV 00 ICN 01

6. Total Attachments: N/A	7. Attachment Numbers - No. of Pages in Each: N/A
------------------------------	--

	Printed Name	Signature	Date
8. Originator	Stephen C. Lu	<i>Pampathi for Stephen Lu</i>	10/06/00
9. Checker	Denny Jones	<i>Pampathi for Denny Jones</i>	10/06/00
10. Lead/Supervisor	Al Lingenfelter	<i>Pampathi for Al Lingenfelter</i>	10/06/00
11. Responsible Manager	Venkataraman Pasupathi	<i>Pampathi</i>	10/06/00

12. Remarks:  
Additional Contributor: David Shoesmith.

**INFORMATION COPY**

**LAS VEGAS DOCUMENT CONTROL**

*WM-11  
NM5507*

Enclosure 2

OFFICE OF CIVILIAN RADIOACTIVE WASTE MANAGEMENT  
ANALYSIS/MODEL REVISION RECORD

*Complete Only Applicable Items*

1. Page: 2 of 32

2. Analysis or Model Title:

Hydrogen Induced Cracking of Drip Shield

3. Document Identifier (including Rev. No. and Change No., if applicable):

ANL-EBS-MD-000006 REV 00 ICN 01

4. Revision/Change No.

5. Description of Revision/Change

00

Initial Issue

00/01

Interim Change Notice to include (1) hydrogen induced cracking due to the possible galvanic contact between the Ti-7 drip shield and steel components that may fall onto the drip shield in the case of a no-backfill drip shield design; and (2) approach to issue resolution status report key technical issue: container life and source term. Changes are indicated by vertical lines in the right margin.

## CONTENTS

	Page
ACRONYMS AND ABBREVIATIONS .....	5
1. PURPOSE.....	6
1.1 PURPOSE AND BACKGROUND.....	6
1.2 RESOLUTION OF COMMENTS IN ISSUE RESOLUTION STATUS REPORT .....	7
2. QUALITY ASSURANCE.....	9
3. COMPUTER SOFTWARE AND MODEL USAGE.....	9
4. INPUTS.....	9
4.1 DATA AND PARAMETERS.....	9
4.2 CRITERIA.....	10
4.3 CODES AND STANDARDS .....	10
5. ASSUMPTIONS.....	11
6. ANALYSIS/MODEL .....	13
6.1 DESCRIPTION OF MODEL FOR HYDROGEN INDUCED CRACKING.....	13
6.1.1 Introduction.....	13
6.1.2 Processes by which Hydrogen is Absorbed .....	14
6.1.3 Critical Hydrogen Concentration, $H_C$ .....	15
6.1.4 Hydrogen Absorption During Crevice Corrosion.....	17
6.1.5 Hydrogen Absorption During General Passive Corrosion.....	18
6.2 APPLICATION OF HIC MODEL TO DRIP SHIELD .....	20
6.2.1 Material .....	20
6.2.2 Determination of the Critical Hydrogen Concentration, $H_C$ .....	21
6.2.3 Determination of Hydrogen Concentration .....	21
6.2.4 Results.....	22
6.2.5 Model Validation .....	23
6.3 HYDROGEN INDUCED CRACKING OF TI-7 DUE TO GALVANIC COUPLE.....	23
6.3.1 Introduction.....	23
6.3.2 Qualitative Assessment.....	24
6.3.3 Mathematical Model for Hydrogen Absorption and Diffusion in DS .....	25
6.3.4 Worst Case Considerations .....	28
7. CONCLUSIONS.....	29
8. INPUTS AND REFERENCES.....	30
8.1 DOCUMENTS CITED .....	30
8.2 CODES, STANDARDS, REGULATIONS, AND PROCEDURES .....	32

## FIGURES

	<b>Page</b>
1. Schematic Showing the Combinations of Stress Intensity Factor and Hydrogen Concentration Leading either to Fast Crack Growth (Brittle Failures) or Slow Crack Growth Due to either Sustained Load Cracking or Ductile Rupture or to No Failure.....	14
2. Hydrogen Concentration in Drip Shield Versus Distance from Contact Area.....	28

## ACRONYMS AND ABBREVIATIONS

AMR	Analyses and Models Report
CLST	container life and source term
CRWMS	Civilian Radioactive Waste Management System
DOE	U.S. Department of Energy
DS	drip shield
EBS	engineered barrier system
GC	general corrosion
HIC	hydrogen induced cracking
HLW	high-level radioactive waste
IRSR	Issue Resolution Status Report
KTI	Key Technical Issue
LC	localized corrosion
M&O	Management and Operating Contractor
MGR	Monitored Geologic Repository
MIC	microbiologically influenced corrosion
NRC	U.S. Nuclear Regulatory Commission
PMR	Process Model Report
QAP	Quality Administrative Procedure
SAW	simulated acidic concentrated water
SCE	saturated calomel electrode
SCW	simulated concentrated water
SDW	simulated dilute water
SNF	spent nuclear fuel
SSW	simulated saturated water
UNS	Unified Numbering System
WP	waste package
WPD	waste package degradation

## 1. PURPOSE

### 1.1 PURPOSE AND BACKGROUND

One likely failure mechanism for titanium and its alloys under repository conditions is via the absorption of atomic hydrogen in the metal crystal lattice. Resulting decreased ductility and fracture toughness may lead to brittle mechanical fracture called hydrogen-induced cracking (HIC) or hydrogen embrittlement. For the current design of the engineered barrier without backfill, HIC may be a problem since titanium drip shield (DS) can be galvanically coupled to carbon steel of the ground support, and rock bolts (or wire mesh) which may fall onto DS, thereby creating conditions for hydrogen production at a faster rate by electrochemical reaction.

The purpose of this scientific analysis and model is to account for the HIC effects on the DS. This Analyses and Models Report (AMR) serves as a feed to the Waste Package Degradation (WPD) Process Model Report (PMR) and was developed in accordance with the activity section "Hydrogen Induced Cracking of Drip Shield" of the development plan entitled *Analysis and Model Reports to Support Waste Package PMR* (CRWMS M&O 1999f).

Titanium Grade 7 (Ti-7) (UNS R52400) is now favored for construction of the drip shield for the waste package due to its excellent corrosion resistance (CRWMS M&O 2000a, Section 1.2). This alloy consists of 0.3% Fe, 0.25% O, 0.12-0.25% Pd, 0.1% C, 0.03% N, 0.015% H, 0.4% total residuals with the balance being Ti (CRWMS M&O 1999d, p. 45). Other titanium alloys that will be discussed in this report include Ti-2, Ti-12, and Ti-16. Ti-2 is essentially commercially pure titanium. It is believed that the most effective way of reducing hydrogen absorption is to choose a more crevice resistant alloy (Shoesmith et al. 1997, p. 15). This improvement in resistance to crevice corrosion can be attributed to the addition of alloying elements, which reinforce passivity. Therefore, susceptibility to crevice corrosion is eliminated through the alloying series Ti-2→Ti-12→Ti-16 (Shoesmith et al. 1997, p. 15). The major additions are Ni (0.6-0.9%) for Ti-12 and Pd (0.04-0.08%) for Ti-16 (CRWMS M&O 1999d, pp. 49, 51). A decrease in the corrosion rate by the addition of a noble metal such as Pd in Ti-16 is noted in Shoesmith et al. (1997, p. 21). The composition of Ti-7 is almost identical to that of Ti-16, but the Pd content is higher in Ti-7 (0.12-0.25%) than in Ti-16 (0.04-0.08%) (CRWMS M&O 1999d, pp. 45, 51). The similarity between Ti-7 and Ti-16 was also noted by CRWMS M&O (2000a, Section 1.2).

The DS will experience a wide range of conditions during its service life (CRWMS M&O 2000a, p. 10). Initially, the underlying high-level waste packages will be relatively hot, and DS surfaces will be dry due to the heat generated from radioactive decay. The temperature will eventually drop to levels where both humid air and aqueous phase corrosion will be possible. Crevice corrosion and slow general passive corrosion will produce hydrogen, which can be absorbed into the metal. In a DS design without backfill, hydrogen generation may be caused by the galvanic couple between the titanium DS surface and structural components (such as rock bolts, wire mesh, and steel liners used in the drift), which may fall onto the DS surface.

HIC of the DS is key to one of the most important principal factors in repository performance—the premature failure of the DS. A realistic model will be used to account for the degradation of

the DS due to the effects of HIC induced by crevice corrosion and general corrosion, based upon data generated by the project. The model will follow the approach of Shoesmith et al. (1997). Both qualitative and quantitative assessments will be conducted to evaluate the effect due to the galvanic couple.

## 1.2 RESOLUTION OF COMMENTS IN ISSUE RESOLUTION STATUS REPORT

As part of the review of site characterization activities, the U.S. Nuclear Regulatory Commission (NRC) has undertaken an ongoing review of information on Yucca mountain site characterization activities to allow early identification and resolution of potential licensing issues. The principal means of achieving this goal is through informal, pre-licensing consultation with the U.S. Department of Energy (DOE). This approach attempts to reduce the number of, and to better define, issues that may be in dispute during the NRC licensing review, by obtaining input and striving for consensus from the technical community, interested parties, and other groups on such issues.

The NRC has focused pre-licensing issue resolution on those topics most critical to the postclosure performance of the potential geologic repository. These topics are called Key Technical Issues (KTIs). Each KTI is subdivided into a number of sub-issues. Early feedback among all parties is essential to define what is known, what is not known and where additional information is likely to make a significant difference in the understanding of future repository safety. The Issue Resolution Status Reports (IRSRs) are the primary mechanism that the NRC staff uses to provide feedback to the DOE on the status of the KTI sub-issues. For most sub-issues, the NRC staff has identified technical acceptance criteria that the NRC may use to evaluate the adequacy of information related to the KTIs.

The primary issue of the KTI on *Issue Resolution Status Report Key Technical Issue: Container Life and Source Term* (NRC 1999) is adequacy of the Engineered Barrier System (EBS) to provide reasonable assurance that containers will be adequately long-lived, and radionuclide releases from the EBS will be sufficiently controlled, and that the container design and packaging of spent nuclear fuel (SNF) and high level radioactive waste (HLW) glass will make a significant contribution to the overall repository performance. The IRSR on Container Life and Source Term (CLST) defines the physical boundary of the EBS by the walls of the WP emplacement drifts. The CLST IRSR deems six sub-issues to be important to the resolution of the relevant KTI. The first sub-issue, the effects of corrosion processes on the lifetime of the containers, and the second sub-issue, the effects of phase instability of materials and initial defects on the mechanical failure and lifetime of the containers, are relevant to this AMR.

The relevant NRC Technical Acceptance Criteria for sub-issues 1, 2, and 6 and the approaches used in this AMR are discussed below:

For sub-issue 1, the effects of corrosion processes on the lifetime of the containers, NRC Technical Acceptance Criteria 1 is "DOE has identified and considered likely modes of corrosion for container materials, including dry-air oxidation, humid-air corrosion, and aqueous corrosion processes, such as GC, LC, MIC, SCC and HIC, as well as the effect of galvanic coupling."

Approach: This AMR includes process-level models for HIC and the effect of galvanic coupling. Other likely models of corrosion for container materials, including dry-air oxidation, humid-air corrosion, and aqueous corrosion processes, such as GC, LC, MIC, and SCC, as well as the effect of galvanic coupling, are dealt with in other companion AMRs.

For sub-issue 2, the effects of phase instability of materials and initial defects on the mechanical failure and lifetime of the containers, NRC Technical Acceptance Criteria 3 is "DOE has demonstrated that the numerical models used for container materials stability and mechanical failures are effective representations, taking into consideration associated uncertainties, of the expected materials behavior and are not likely to underestimate the actual rate of failure in the repository environment."

Approach: Uncertainties, assumptions, and limitations of the process level models associated with HIC and the effect of galvanic coupling are addressed in this AMR. Other likely models are dealt with in other companion AMRs.

For sub-issue 6, the effects of alternate engineered barrier subsystem design features on container lifetime and radionuclide release from the engineered barrier subsystem, NRC Technical Acceptance Criteria 1 is "DOE identified and considered the effects of backfill, and the timing of its emplacement, on the thermal loading of the repository, WP lifetime (including container corrosion and mechanical failure), and the release of radionuclides from the EBS."

Approach: REV00 of this AMR was prepared to address HIC on the DS as a part of the EBS based on the design which considers the effects of backfill. The current version of the AMR incorporates changes, which are necessary for an alternative design without the effects of backfill. In a DS design without backfill, hydrogen generation may be caused by the galvanic couple between the titanium DS surface and structural components (such as rock bolts, wire mesh, and steel liners used in the drift) which may fall on the DS surface. Both qualitative and quantitative assessments are included in this AMR to evaluate the effect due to the galvanic couple.

For sub-issue 6, the effects of alternate engineered barrier subsystem design features on container lifetime and radionuclide release from the engineered barrier subsystem, NRC Technical Acceptance Criteria 4 is "DOE has identified and considered the effects of drip shields (with backfill) on WP lifetime, including extension of the humid-air corrosion regime, environmental effects, breakdown of drip shields and resulting mechanical impacts on WP, the potential for crevice corrosion at the junction between the WP and the drip shield, and the potential for condensate formation and dripping on the underside of the shield."

Approach: See approach for sub-issue 6, NRC Technical Acceptance Criteria 1 above.

## 2. QUALITY ASSURANCE

The Quality Assurance (QA) program applies to this AMR. All types of waste packages (WPs) were classified (per QAP-2-3) as Quality Level-1. CRWMS M&O (1999a, p. 7), *Classification of the MGR Uncanistered Spent Nuclear Fuel Disposal Container System*, is cited as an example of a WP type. The development of this AMR is conducted under activity evaluation *1101213PM7 Waste Package Analysis & Models - PMR* (CRWMS M&O 1999e), which was prepared per QAP-2-0. Note that QAP-2-0, *Conduct of Activities*, has been superseded by AP-2.21Q, *Quality Determinations and Planning for Scientific, Engineering, and Regulatory Compliance Activities*; however, the Activity Evaluation remains in effect. The results of that evaluation were that the activity is subject to the *Quality Assurance Requirements and Description* (DOE 2000) requirements. According to the development plan of this AMR (CRWMS M&O 1999f), no special controls on the electronic management of data are applicable in this activity.

## 3. COMPUTER SOFTWARE AND MODEL USAGE

No computer software or models have been used to support the development of the analysis activities described in this AMR.

## 4. INPUTS

### 4.1 DATA AND PARAMETERS

The following input data and/or parameters are obtained from Shoesmith et al. (1997, pp. 7-11):

$H_C$  = critical hydrogen concentration.

The following input data and/or parameters are obtained from Shoesmith et al. (1997, p. 22):

$f_h$  = fraction of absorption efficiency.

The following input data and/or parameters are obtained from Weast and Astle (1978, p. B-177):

$\rho_{Ti}$  = density of titanium

$M_{Ti}$  = Molecular weight of titanium

$\rho_{OX}$  = density of titanium oxides

$M_{OX}$  = Molecular weight of titanium oxides.

The following input data and/or parameters for Ti-7 are obtained from CRWMS M&O (2000a, Section 6.4.3):

$E_{corr}$  = the open circuit corrosion potential

$E_{critical}$  = the threshold potential for breakdown of the passive film.

The following input data and/or parameters for Ti-7 are obtained from CRWMS M&O (2000a, Section 6.5.4):

$R_{uc}$  = passive general corrosion rate (50<sup>th</sup> percentile, 90<sup>th</sup> percentile and maximum).

All of these input data and parameters will be used to evaluate the HIC effects on the DS.

## 4.2 CRITERIA

The DS is intended to protect the WP, thereby prolonging WP life. Therefore, the DS must help meet criteria specific to the WP.

In addition to the criteria specifically relevant to the WP, criteria for the DS have now been developed. *Emplacement Drift System Description Document* (SDD-EDS-SE-000001) (CRWMS M&O 2000b), Design Criteria 1.2.1.12 and 1.2.1.18, in the emplacement drift SDD (pp. 10-11), which uses 10 CFR 63 and EDA II as its framework, appear to be the best candidates in supporting this analysis.

The criterion 1.2.1.12 states:

“The drip shield shall have an operating life of 10,000 years.”

The criterion 1.2.1.18 states:

“The drip shield material shall be Grade 7 Titanium, a minimum of 15-mm thick at the time of emplacement.”

These criteria are needed to ensure that the drip shield is designed with an operating life long enough to achieve the functions allocated to it.

## 4.3 CODES AND STANDARDS

No codes or standards were used to perform the analysis for this AMR.

## 5. ASSUMPTIONS

The following assumptions are for the HIC model of this AMR:

- 5.1 Due to the close similarity in chemical composition between Ti-7 and Ti-16, available material property data for Ti-16 are assumed to be applicable to Ti-7 if the said material property data are not available for Ti-7. This assumption is used in Sections 6.1 and 6.2.
- 5.2 The  $H_C$  value for Ti-7 is assumed to be at least 1000  $\mu\text{g/g}$ . This assumption is based on Assumption 5.1 and data reported by Ikeda and Quinn (1998, p. 7), which indicated that the  $H_C$  value for Ti-16 is between 1000 and 2000  $\mu\text{g/g}$ . This assumption is necessary because  $H_C$  data are not available for Ti-7. This value appears excessively conservative on a number of counts: (1) the value of 400  $\mu\text{g/g}$  is the lower limit of the measured range of 400 to 1000  $\mu\text{g/g}$  measured at room temperature ( $\sim 25^\circ\text{C}$ ) for Ti-2 (Shoesmith et al. 1997, p 7-11); (2) the temperature of the drip shield will be well above this value for the majority of its anticipated lifetime and Clarke et al. (1995) have shown  $H_C$  for both Ti-2 and Ti-12 rises to  $\sim 1000\mu\text{g/g}$  at a temperature of  $92^\circ\text{C}$  to  $100^\circ\text{C}$ ; and (3) the value of 400  $\mu\text{g/g}$  was measured for Ti-2, whereas the value for Ti-16, a palladium containing alpha alloy with similar properties to Ti-7, appears to be  $> 1000 \mu\text{g/g}$  ( Ikeda and Quinn 1998, p.7). This assumption is used in Subsections 6.1.3 and 6.2.2.

It is noted that 400  $\mu\text{g/g}$ , the lower bound value observed for other titanium alloys (e.g., Ti-2 and Ti-12) by Shoesmith et al. (1997, pp. 7-11), was used as the critical hydrogen concentration for Ti-7 in REV00 of this AMR. As discussed above, this value appears to be excessively conservative based on data reported by Ikeda and Quinn (1998, p. 7).

- 5.3 Mechanisms for hydrogen generation and absorption on a titanium surface may include a galvanic couple, hydrogen produced in atomic form by the corrosion process, and the direct absorption of hydrogen produced by water radiolysis. As indicated by Shoesmith et al. (1997, p. 17), the direct absorption of radiolytically produced hydrogen is insignificant except at high dose rate ( $> 10^2 \text{ Gy/h}$ ) and high temperature ( $> 150^\circ\text{C}$ ), clearly unattainable under Yucca Mountain DS conditions. Therefore, only galvanic couple and generation and absorption of corrosion produced hydrogen are considered in this AMR. This assumption is used in Subsections 6.1.2 and 6.1.5.
- 5.4 The film growth rate and, hence, the corrosion rate are assumed to be constant in time for the formula used to calculate the concentration of hydrogen in the metal (Shoesmith et al. 1997, p. 22). The rationale for this assumption is that the assumption of constant corrosion rate is conservative and less conservative corrosion models assume that the rate decays with time (CRWMS M&O 2000a, Section 5.3). It is also implicit in this assumption and this formula that any hydrogen absorbed into the titanium remains within the remaining wall thickness and is not subsequently removed as the general corrosion process progresses with time. This is a very conservative assumption, since any titanium hydride formed within the alloy will be unstable with respect to titanium oxide (Beck 1973) and should,

therefore, be removed by the general corrosion process. This assumption is used in Subsections 6.1.5 and 6.2.3.

5.5 A mathematical model is proposed in Section 6.3.3 to predict the hydrogen concentration in the DS due to a galvanic couple between the DS and a carbon steel segment. Simplifying assumptions are employed to develop the mathematical model. Because the assumptions are to simplify the system for the mathematical model, they do not require a technical basis or verification. These assumptions are:

- The DS is treated as an infinite flat plate. This is a conservative assumption in such a way that a larger surface area is available for galvanic coupling between the DS and a carbon steel segment than a curved DS structure. This assumption is also to simplify the geometry for the mathematical model.
- The contact plane between the DS surface and the carbon steel segment is circular in shape. This assumption is also to simplify the geometry for the mathematical model.
- Hydrogen is absorbed into the DS through the contact plane and immediately reaches the other surface. The initial region of the DS with hydrogen absorption has the shape of a circular disk. This assumption is also to simplify the geometry for the mathematical model.
- As hydrogen starts to diffuse in the DS, the radius of the circular region will expand at a constant speed  $v$ . This assumption is also to simplify the geometry for the mathematical model.

## 6. ANALYSIS/MODEL

### 6.1 DESCRIPTION OF MODEL FOR HYDROGEN INDUCED CRACKING

#### 6.1.1 Introduction

The DS will experience a wide range of conditions during its service life (CRWMS M&O 2000a, Section 1.3). Initially, the underlying high-level waste packages will be relatively hot, and DS surfaces will be dry due to the heat generated from radioactive decay. The temperature will eventually drop to levels where both humid air and aqueous phase corrosion will be possible. Crevice corrosion and slow general passive corrosion may be initiated and propagate in the metal. Both types of corrosion will produce hydrogen, which can be absorbed into the metal (Shoesmith et al. 1997, p. 2). In a DS design without backfill, hydrogen generation may be caused by the galvanic couple between the titanium DS surface and structural components (such as rock bolts, wire mesh, and steel liners used in the drift), which may fall onto the DS surface.

Failure occurs if (1) the wall penetration by corrosion exceeds the corrosion allowance or (2) the amount of hydrogen absorbed exceeds the critical hydrogen concentration,  $H_C$ , for failure due to hydrogen induced cracking. The first type of failure mechanism, i.e., wall penetration by crevice and general corrosion, is treated in another AMR (CRWMS M&O 2000a). This AMR deals with the failure mechanism associated with HIC.

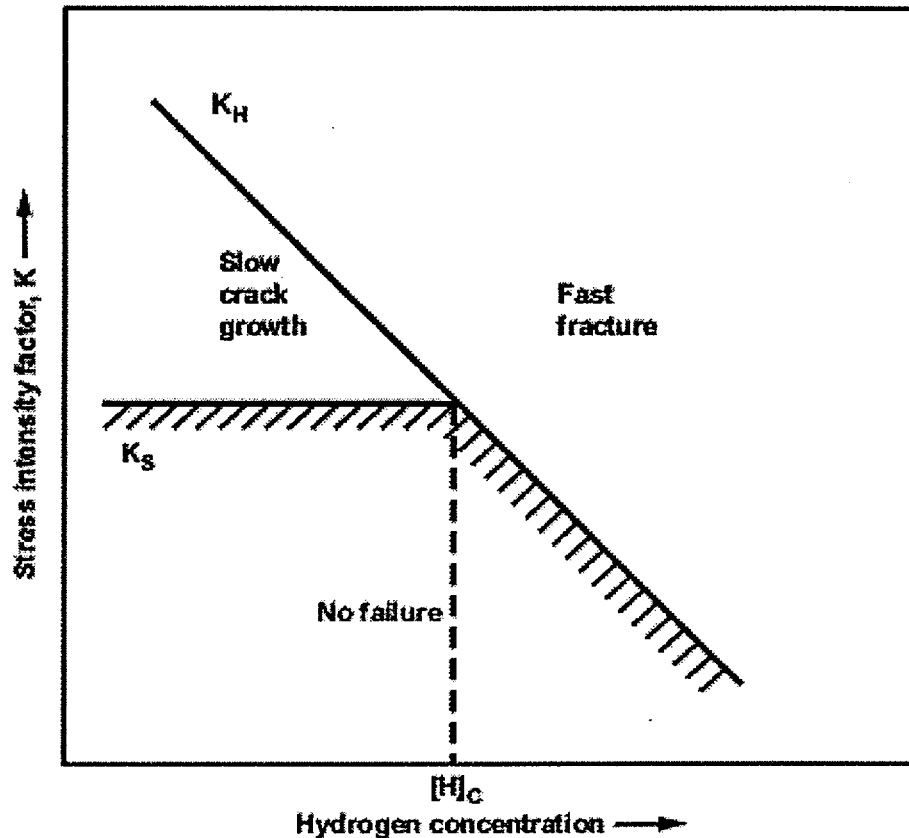
HIC (also called hydrogen embrittlement) is characterized by decreased fracture toughness or ductility of the metal due to absorbed atomic hydrogen. The usual mechanical failure mode for a ductile material is the ductile tearing observed during slow crack growth. Decreased fracture toughness causes fast crack growth (brittle fracture) of a normally ductile material under sustained load. During slow crack growth, material will fail as the stress intensity factor  $K$  reaches a value  $K_S$ . During fast crack growth, the same material will fail as the stress intensity factor  $K$  reaches a value  $K_H$ , which is less than  $K_S$  (Shoesmith et al. 1997). Figure 1 (from Shoesmith et al. 1997, page 9, Figure 7) represents, schematically, the combinations of stress intensity factor and hydrogen concentration leading to (1) fast crack growth (brittle fracture) controlled by  $K_H$ , (2) slow crack growth controlled by  $K_S$  due to either sustained load cracking or ductile rupture, or (3) no failure.

For corrosion induced HIC, an approach has been adopted to predict when HIC might become a potential failure process for the DS, following a Canadian precedent (Shoesmith et al. 1997). The basic premise of the model is that failure will occur once the hydrogen content exceeds a certain limit or critical value. Both qualitative and quantitative assessments will be conducted to evaluate the effect due to the galvanic couple.

This report will address:

- Processes by which Ti-7 can absorb hydrogen and, hence, eventually become susceptible to HIC
- Analysis procedures for predicting the consequences of hydrogen absorption

- Acquisition of input data for the analysis parameters
- Results.



SL\_AMR1\_figB-1

NOTE: Shoesmith et al. (1997)

Figure 1. Schematic Showing the Combinations of Stress Intensity Factor and Hydrogen Concentration Leading either to Fast Crack Growth (Brittle Failures) or Slow Crack Growth Due to either Sustained Load Cracking or Ductile Rupture or to No Failure

### 6.1.2 Processes by which Hydrogen is Absorbed

In accordance with Schutz and Thomas (1987, p. 673), factors have been identified that can lead to HIC, i.e., hydrogen uptake and possible embrittlement of  $\alpha$  and near- $\alpha$  titanium alloys (such as titanium grade 2, grade 7 and grade 12) in aqueous media. The three general conditions that must exist simultaneously for the hydrogen embrittlement of  $\alpha$  alloys are:

- A mechanism for generating hydrogen on a titanium surface. The mechanisms may include a galvanic couple, hydrogen produced in atomic form by the corrosion process, and the direct absorption of hydrogen produced by water radiolysis. As indicated in Section 5 (Assumption

5.3), the direct absorption of radiolytically produced hydrogen is insignificant except at high dose rate ( $> 10^2$  Gy/h) and high temperature ( $> 150^\circ\text{C}$ ), clearly unattainable under Yucca Mountain DS conditions. Therefore, only hydrogen produced by a galvanic couple and general corrosion are considered in this AMR.

- Metal temperature above approximately  $80^\circ\text{C}$  ( $175^\circ\text{F}$ ), where the diffusion rate of hydrogen into  $\alpha$  titanium is significant.
- Solution pH less than 3 or greater than 12, or impressed potentials more negative than  $-0.7$  V(SCE).

Assessment of HIC due to effects of a galvanic couple will be presented in Section 6.3. The remaining of Section 6.1 and Section 6.2 will be devoted to HIC resulting from hydrogen produced by corrosion of titanium.

Both crevice corrosion and general passive corrosion will be accompanied by hydrogen production and, hence, possibly by the absorption of hydrogen into the metal.

For crevice corrosion the hydrolysis of dissolved metal cations leads to acidification within the occluded area and the development of active conditions in which the metal is unprotected by an oxide film. Once initiated, crevice corrosion is supported by both the reduction of oxygen on passive surfaces external to the crevice and the reduction of protons ( $\text{Ti} + 4\text{H}^+ \rightarrow \text{Ti}^{++} + 2\text{H}_2$ ) on exposed metal surfaces inside the crevice. The latter process can lead to the absorption of atomic hydrogen into the metal in sufficient quantities to produce extensive hydride formation (Shoesmith et al. 1997, Figure 3, p. 4).

For the passive non-creviced or the repassivated crevice conditions expected to prevail, the corrosion of the titanium alloy will be sustained by reaction with water under neutral conditions ( $\text{Ti} + 2\text{H}_2\text{O} \rightarrow \text{TiO}_2 + 2\text{H}_2$ ) and will proceed at an extremely slow rate. This process will generate hydrogen, which must pass through the  $\text{TiO}_2$  film before absorption in the underlying Ti alloy can produce HIC. Redox transformations ( $\text{Ti}^{\text{IV}} \rightarrow \text{Ti}^{\text{III}}$ ) in the film are required before the oxide becomes significantly transparent to hydrogen. Significant cathodic polarization of the metal (generally only achievable by galvanic coupling to carbon steel or the application of a cathodic protection potential) is required for these transformations to occur. Measurements of absorbed hydrogen suggest a threshold potential of  $-0.6$  V versus saturated calomel electrode (SCE) above which no absorption occurs (Shoesmith et al. 1997, p. 4). Only impressed current cathodic protection or galvanic coupling to active alloys of Fe, Zn, or Mg could readily produce such active potential. Thus, hydrogen generation rates, and, hence, hydrogen absorption rates, are expected to be very low on Ti alloy surfaces.

### 6.1.3 Critical Hydrogen Concentration, $H_C$

Provided that wall penetration by corrosion does not exceed the corrosion allowance, HIC failure is assumed to occur when the material has absorbed enough hydrogen to exceed the critical hydrogen content,  $H_C$ . Observations regarding the critical hydrogen content,  $H_C$ , for Ti-2 and Ti-12 (Shoesmith et al. 1997, pp. 7-11) are summarized as follows:

Using the slow strain rate technique on precracked compact tension specimens precharged with known amounts of hydrogen, it has been shown that the fracture toughness of Ti-2 and Ti-12 is not significantly affected until hydrogen content exceeds  $H_C$ . Once above  $H_C$ , there is no slow crack growth, and only fast crack growth is observed.

$H_C$  is sensitive to the microstructure and texture of the material with respect to the orientation of the crack and the applied stress. Preferential pathways for cracking are formed along  $\beta$ -phase stringers introduced through the manufacturing process. An  $H_C$  of 500  $\mu\text{g/g}$  has been measured in Ti-12 containing cracks propagating in the directions defined by these stringers. Crack propagation perpendicular to these features is not observed up to  $H_C = 2000 \mu\text{g/g}$ . Heat treatment to remove this laminar structure by randomly reorienting the residual  $\beta$ -phase can lead to a decrease in  $H_C$  to  $\sim 400 \mu\text{g/g}$ .

Even for manufactured plate materials that do not have high  $\beta$ -phase content, e.g., Ti-2, the laminar structure introduced by rolling appears to dominate the cracking behavior. As a consequence, depending on crack orientation,  $H_C$  varies between  $\sim 400$  and  $1000 \mu\text{g/g}$ . Since Ti-2 does not contain as much  $\beta$ -phase as Ti-12, heat treatment does not exert a significant influence on  $H_C$ . Welding produces a larger change in the microstructure than does heat treatment. The high weld temperature results in significant microstructural changes in the weldment. This results in a small decrease in strength. The heat affected zone does not appear to be sufficiently large to influence the cracking behavior because, for both Ti-2 and Ti-12,  $H_C$  is slightly decreased near the weld metal compared to the base metal. It did not decrease below  $500 \mu\text{g/g}$ .

It can also be assumed that failure is less likely at elevated temperature. This assumption is justified, in part, by recognizing that the hydrogen solubility would be higher at elevated temperature. However, it has also been shown experimentally that  $H_C$  increases markedly with temperature (Clarke et al. 1995). While the maximum critical stress intensity factor for Ti-2 decreases slightly from  $\sim 50 \text{ MPa/m}^{1/2}$  to  $\sim 40 \text{ MPa/m}^{1/2}$  at  $95^\circ\text{C}$ , only slow crack growth was observed up to hydrogen concentrations of  $\sim 2000 \mu\text{g/g}$ , clearly indicating an enhanced resistance to growth of brittle-like cracks as the temperature is increased. A similar increase in resistance to brittle fracture was observed for Ti-12 at  $95^\circ\text{C}$ , the maximum stress intensity factor decreasing from  $\sim 60 \text{ MPa/m}^{1/2}$  to  $\sim 45 \text{ MPa/m}^{1/2}$ , while  $H_C$  increased to  $\sim 1000 \mu\text{g/g}$  (Clarke et al. 1995). Preliminary creep measurements clearly indicate that increased creep deformation at higher temperatures was a major factor in preventing the development of a sufficiently high stress concentration to initiate fast fracture (Clarke et al. 1995).

$H_C$  data are not available for Ti-7 but more recent data reported by Ikeda and Quinn (1998, p. 7) indicated that the  $H_C$  value for Ti-16 is between  $1000$  and  $2000 \mu\text{g/g}$ . As noted in Section 1, Ti-7 and Ti-16 are similar alloys because of their similar chemical compositions.

The  $H_C$  value for Ti-7 is assumed to be at least  $1000 \mu\text{g/g}$ . This assumption is based on Assumption 5.1 and data reported by Ikeda and Quinn (1998, p. 7), which, as indicated earlier, concluded that the  $H_C$  value for Ti-16 is between  $1000$  and  $2000 \mu\text{g/g}$ . This assumption is necessary because  $H_C$  data are not available for Ti-7.

It is noted that 400 µg/g, the lower bound value observed for other titanium alloys (e.g., Ti-2 and Ti-12) by Shoesmith et al. (1997, pp. 7-11) was used as the critical hydrogen concentration for Ti-7 in REV00 of this AMR. This value appears to be excessively conservative based on data reported by Ikeda and Quinn (1998, p. 7).

#### 6.1.4 Hydrogen Absorption During Crevice Corrosion

Crevice corrosion, if it initiates, will propagate at a rate much higher than that of general corrosion. Crevice propagation, as mentioned in Section 6.1.1, can lead to failure by wall penetration as well as failure due to HIC because of hydrogen transported into the metal.

The most effective way to reduce hydrogen absorption is to choose a more crevice corrosion resistant alloy (Shoesmith et al. 1997, p. 15). Improvements in resistance to crevice corrosion have been attributed to alloying elements, which reinforce passivity. Susceptibility to crevice corrosion is eliminated through the alloying series Ti-2→Ti-12→Ti-16 (Shoesmith et al. 1997, p. 15). In accordance with CRWMS M&O (1999d, pp. 49, 51), the major additions are Mo (0.2-0.4%) and Ni (0.6-0.9%) for Ti-12 and Pd (0.04-0.08%) for Ti-16. Decreased crevice corrosion rates by adding alloying elements such as Mo and Ni to Ti-12 and Pd to Ti-16 are noted in Shoesmith et al. (1997, p.16), and discussed in recent reviews of Ti crevice corrosion behavior (Schutz 1988). The effect of deliberate alloying of Ti-12 with Ni and Mo, which segregate at grain boundaries and intermetallics, is to improve the susceptibility to crevice corrosion from repassivation after some crevice corrosion in Ti-2 to repassivation after minor crevice corrosion damage in Ti-12. The effect of adding Pd to ennoble titanium while avoiding segregation in Ti-16 is to further improve the susceptibility to crevice corrosion from repassivation after minor crevice corrosion in Ti-12 to no crevice corrosion damage in Ti-16. It can be seen from CRWMS M&O (1999d, pp. 45, 51) that the composition of Ti-7 is almost identical to that of Ti-16, but the Pd content is even higher in Ti-7 (0.12-0.25%) than in Ti-16 (0.04-0.08%). Therefore, Ti-7, like Ti-16, is not expected to suffer any crevice damage.

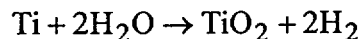
Crevice corrosion is one form of localized corrosion of a metal surface (ASM 1987, p. 4). The localized corrosion model developed by CRWMS M&O (2000a, Section 6.4.1) for Ti-7 DS assumes that localized attack occurs only if the open circuit corrosion potential,  $E_{corr}$ , exceeds the threshold potential for breakdown of the passive film,  $E_{critical}$ . Experimental measurements reported by CRWMS M&O (2000a, Section 6.4.3) for  $E_{corr}$  and  $E_{critical}$  were obtained from various test environments expected in the repository. These test environments include simulated dilute water (SDW), simulated concentrated water (SCW), and simulated acidic concentrated water (SAW) at 30, 60, and 90°C, as well as simulated saturated water (SSW) at 100 and 120°C. SCW is about one thousand times more concentrated than J-13 well water and is slightly alkaline (pH~8). SAW is about one thousand times more concentrated than J-13 well water and is acidic (pH~2.7). J-13 well water (Harrar et al. 1990) is the groundwater at some distance from Yucca Mountain. The experimental measurements show that the threshold  $E_{critical}$  is consistently greater than  $E_{corr}$ . CRWMS M&O (2000a, Section 6.4.3) indicated that the difference,  $E_{critical} - E_{corr}$ , falls in the range from 500 mV to 1650 mV for the various test environments of SDW, SCW, SAW, and SSW at temperature from 20-150°C.

It is, therefore, concluded that hydrogen absorption during crevice corrosion may be ignored in the HIC model.

### 6.1.5 Hydrogen Absorption During General Passive Corrosion

According to Shoesmith et al. (1997, p. 15), there are two processes by which hydrogen could be produced, and possibly absorbed, under passive conditions: (1) direct absorption of hydrogen produced by water radiolysis and (2) absorption of atomic hydrogen produced by the corrosion process to produce oxide. The direct absorption of radiolytically produced hydrogen does not appear to be significant except at high dose rate ( $> 10^2$  Gy/h) and high temperature ( $> 150^\circ\text{C}$ ) (Shoesmith et al. 1997, p. 17). This condition is clearly unattainable under Yucca Mountain DS conditions and will not be considered, leaving the corrosion process as the only feasible source of hydrogen for absorption.

Under anoxic conditions, when passive corrosion should prevail, the corrosion potential for passive titanium must reside at a value at which water reduction can couple to titanium oxidation,



and, hence, must be at, or more negative than, the thermodynamic stability line for water. At such potentials, titanium hydrides are thermodynamically stable with respect to the metal. Consequently the passive film can be considered only as a transport barrier and not as an absolute barrier. The rate of hydrogen absorption at the corrosion potential will be controlled by the rate of the corrosion reaction, which dictates the rate of production of absorbable hydrogen. Since titanium oxide,  $\text{TiO}_2$ , is extremely stable and protective in the DS environment, the corrosion reaction will be effectively limited to an oxide film growth reaction.

While the rate of hydrogen production and, hence, absorption may be assumed directly proportional to the rate of film growth, the fraction of hydrogen absorption needs to be determined. Based on available test data, Shoesmith et al. (1997, p. 22) suggests the use of 0.1 and 0.02 for fractional efficiency for absorption values,  $f_H$ , to represent high and low hydrogen absorption efficiencies for titanium alloys. The high value of 0.1 was obtained by direct analysis of the amount of hydrogen absorbed during crevice corrosion and is, therefore, not an appropriate value to use for T-7 which is immune to crevice corrosion under repository conditions. In their conservative and bounding calculations, Shoesmith et al. (1997, p.22) used this value for Ti-12, since the influence on hydrogen absorption of the presence of  $\text{Ti}_2\text{Ni}$  intermetallics and Ni-stabilized  $\beta$ -phase in this alloy was not known. The lower value of 0.02 was adopted from the experimental measurements of Okada (1983) and can be considered a very conservative value since it was measured on Ti-2 under constant applied current conditions with an applied current of  $0.5 \text{ mA/cm}^2$  at  $25^\circ\text{C}$  in sodium sulphate solutions ( $\text{pH} = 4$ ). The electrode potential achieved during these experiments was  $-1.14 \text{ V}$  (vs. SCE), about  $-0.5 \text{ V}$  more negative than the threshold value of  $-0.6 \text{ V}$  (vs SCE) for hydrogen absorption. Similar measurements on Pt and Ni-coated Ti-2 specimens gave a value of  $f_H$  only marginally higher under these conditions, a clear indication that the Pd-content of Ti-7 would not be expected to increase this value. The applied current density used was  $500 \text{ } \mu\text{A/cm}^2$  compared to a value of  $1.45 \text{ nA/cm}^2$

calculated as the current which would flow at a general corrosion rate of 50 nm/year (the 70<sup>th</sup> percentile value of general corrosion rates measured for Ti-7 in the LTCTF at Lawrence Livermore National Laboratories (CRWMS M & O 2000a, Section 6.5.4). This lower value has been used for Ti-7.

The low value would appear most appropriate for Ti-2 since the passive film is a good transport barrier to hydrogen absorption. For Ti-12, since Ni, in either Ti<sub>2</sub>Ni intermetallics or in β phase, is present, the higher value would be more conservative. For Ti-16 in which intermetallic formation is avoided, the lower value is appropriate. The lower value should also be used for Ti-7 because of the similarity in chemical composition between Ti-7 and Ti-16.

Based on a constant film growth rate and, hence, the corrosion rate, Shoesmith et al. (1997, p. 22) indicated that the concentration of hydrogen in the metal, H<sub>A</sub>, in g/mm<sup>3</sup> can be calculated as a function of time of emplacement (t in years) from the expression:

$$H_A = 4(\rho_{Ti}/10^3)f_h R_{uc} t [M_{Ti}(d_o - R_{uc}t)]^{-1} \quad (\text{Eq. 1})$$

where

$H_A$  = hydrogen content (g/mm<sup>3</sup>)

$\rho_{Ti}$  = density of Ti (g/cm<sup>3</sup>) = 4.5 (Weast and Astle 1978, p. B-177)

$f_h$  = fractional efficiency for absorption

$R_{uc}$  = rate of general passive corrosion (mm/year)

$t$  = time of emplacement in years

$M_{Ti}$  = atomic mass of Ti = 47.9 (Weast and Astle 1978, p. B-177)

$d_o$  = original corrosion allowance (mm) = container wall thickness

The fractional efficiency for absorption, based on previous discussion, is  $f_h = 0.02$  for Ti-7.

Considering a Ti-7 plate with 1 mm<sup>2</sup> surface area, it is noted in Equation 1 that: (1) hydrogen in grams produced by the general corrosion after t years of emplacement is  $4(\rho_{Ti}/10^3)R_{uc}t/M_{Ti}$  based on the reaction  $Ti + 2H_2O \rightarrow TiO_2 + 2H_2$ ; (2) multiplication by the factor  $f_h$  converts the produced hydrogen into absorbed hydrogen; and (3) the remaining volume of Ti-7 alloy in mm<sup>3</sup> is presented by  $(d_o - R_{uc}t)$ . The derivation of Equation 1 is based on a constant general corrosion rate. It was noted by CRWMS M&O (2000a, p. 48) that the assumption of constant corrosion rate is conservative, and less conservative corrosion cases assume that the rate decays with time. It was also noted above that it is conservative to assume that all the hydrogen absorbed during general corrosion is retained within the remaining drip shield wall thickness as

the general corrosion process proceeds. It is most likely that the majority of it will be removed by conversion to the more thermodynamically stable titanium oxide as corrosion progresses.

Using the relationship  $H$  ( $\mu\text{g}$  of  $\text{H}/\text{g}$  of  $\text{Ti}$ ) =  $H$  ( $\text{g}$  of  $\text{H}/\text{mm}^3$  of  $\text{Ti}$ )( $1000/(10^{-6}/\rho_{\text{Ti}})$ ), Equation 1 can be rewritten for  $H_A$  in  $\mu\text{g}/\text{g}$  as follows:

$$H_A = 4 \times 10^6 f_h R_{uc} t [M_{\text{Ti}}(d_o - R_{uc}t)]^{-1} \quad (\text{Eq. 2})$$

where

$H_A$  = hydrogen content ( $\mu\text{g}/\text{g}$ )

The rate of general passive corrosion,  $R_{uc}$ , can be calculated from the rate of oxide film thickness,  $R_{ox}$  by the following formula:

$$R_{uc} = R_{ox} (\rho_{ox} / M_{ox}) (\rho_{\text{Ti}} / M_{\text{Ti}})^{-1} \quad (\text{Eq. 3})$$

where

$\rho_{ox}$  = density of the oxide in  $\text{g}/\text{cm}^3$

$M_{ox}$  = molecular mass of the oxide

since the value of  $(\rho_{ox} / M_{ox}) (\rho_{\text{Ti}} / M_{\text{Ti}})^{-1}$  is always greater than unity, it is conservative to assume that  $R_{uc} = R_{ox}$ .

The general corrosion rates reported in CRWMS M&O (2000a, Section 6.5.4) have been used. The rate at the 50<sup>th</sup> percentile is approximately 25nm/year; the rate at the 90<sup>th</sup> percentile is approximately 100 nm/year; and the maximum rate is less than 350 nm/year.

## 6.2 APPLICATION OF HIC MODEL TO DRIP SHIELD

### 6.2.1 Material

Titanium Grade 7 (Ti-7) (UNS R52400) is now being considered for construction of the DS for the WP. As indicated in Section 1, this alloy consists of 0.3% Fe, 0.25% O, 0.12-0.25% Pd, 0.1% C, 0.03% N, 0.015% H, and 0.4% total residuals with the balance being Ti.

Both crevice corrosion and general passive corrosion will be accompanied by hydrogen production and, hence, possibly by the absorption of hydrogen into the metal. It has been concluded in Section 6.1.4 that hydrogen absorption during crevice corrosion will not be considered in the HIC model since crevice corrosion is essentially eliminated for Ti-7.

General corrosion rates for Ti-16 reported by CRWMS M&O (2000a, Section 6.5.4) indicated that the rate at the 50<sup>th</sup> percentile is approximately 25nm/year (or  $25 \times 10^{-6}$  mm/year); the rate at the 90<sup>th</sup> percentile is approximately 100 nm/year (or  $100 \times 10^{-6}$  mm/year); and the maximum rate is less than 350 nm/year.

### 6.2.2 Determination of the Critical Hydrogen Concentration, $H_C$

As discussed in Section 6.1.3, Shoesmith et al. (1997, p. 11) concluded that a conservative value of  $H_C = 500 \mu\text{g/g}$  can be adopted as the critical hydrogen concentration in rolled plate material using Ti-2 and Ti-12 for predicting container lifetime. The lowest  $H_C$  value observed for Ti-2 and Ti-12 is  $\sim 400 \mu\text{g/g}$ . Ikeda and Quinn (1998) indicated that  $H_C$  for Ti-16 is at least  $1000 \mu\text{g/g}$  and may be much greater.

The  $H_C$  value for Ti-7 is assumed to be at least  $1000 \mu\text{g/g}$ . This assumption is based on Assumption 5.1 and data reported by Ikeda and Quinn (1998, p. 7), which, as indicated earlier, concluded that the  $H_C$  value for Ti-16 is between 1000 and  $2000 \mu\text{g/g}$ . This assumption is necessary because  $H_C$  data are not available for Ti-7.

It is noted that  $400 \mu\text{g/g}$ , the lower bound value observed for other titanium alloys (e.g., Ti-2 and Ti-12) by Shoesmith et al. (1997, pp. 7-11), was used as the critical hydrogen concentration for Ti-7 in REV00 of this AMR. This value appears to be excessively conservative based on data reported by Ikeda and Quinn (1998, p. 7).

### 6.2.3 Determination of Hydrogen Concentration

Based on Equation 2, the hydrogen concentration in the metal can be rewritten as follows:

$$H_A = 4 \times 10^6 f_h R_{uc} t [M_{Ti} (d_o - R_{uc} t)]^{-1}$$

where

$H_A$  = hydrogen content ( $\mu\text{g/g}$ )

$\rho_{Ti}$  = density of Ti in  $\text{g/cm}^3 = 4.5$  (Weast and Astle 1978, p. B-177)

$f_h$  = fractional efficiency for absorption

$R_{uc}$  = rate of general passive corrosion (mm/year)

$t$  = time of emplacement in years

$M_{Ti}$  = atomic mass of Ti = 47.9 (Weast and Astle 1978, p. B-177)

$d_o$  = original corrosion allowance (mm) = container wall thickness

The fractional efficiency for absorption, based on previous discussion, is  $f_h = 0.02$  for Ti-7. The rate of general passive corrosion is  $R_{uc} = 100 \times 10^{-6}$  mm/year (90<sup>th</sup> percentile value) or  $25 \times 10^{-6}$  mm/year (50<sup>th</sup> percentile value) based on Section 6.2.1. The time of emplacement is  $t = 10,000$  years. One half of the minimum wall thickness (15 mm) is assumed for  $d_o$ , i.e.,  $d_o = 7.5$  mm.

#### Case 1: Conservative Estimate

$$R_{ox} = 100 \times 10^{-6} \text{ mm/year (90}^{\text{th}} \text{ percentile value, CRWMS M\&O (2000a, Section 6.5.4))}$$

$$f_h = 0.02$$

$$d_o = 7.5 \text{ mm}$$

$$t = 10,000 \text{ years}$$

From Equation 2,  $H_A = 257 \mu\text{g/g} < H_c = 1000 \mu\text{g/g}$ .

#### Case 2: Best Estimate

$$R_{ox} = 25 \times 10^{-6} \text{ mm/year (50}^{\text{th}} \text{ percentile value, CRWMS M\&O (2000a, Section 6.5.4))}$$

$$f_h = 0.02$$

$$d_o = 7.5 \text{ mm}$$

$$t = 10,000 \text{ years}$$

From Equation (2),  $H_A = 58 \mu\text{g/g} < H_c = 1000 \mu\text{g/g}$ .

### 6.2.4 Results

The analytical estimate presented in Section 6.2.3 based on Equation 2 indicated that there exists a big margin of safety for the drip shield against the effects of HIC. The hydrogen concentration in the DS at 10,000 years after emplacement is  $257 \mu\text{g/g}$  resulting from a conservative estimate and  $58 \mu\text{g/g}$  from a best estimate. The estimated hydrogen concentration in either case is less than the critical hydrogen concentration of  $1000 \mu\text{g/g}$  for Ti-7.

As discussed in Section 6.1.5, the current model is highly conservative in that it assumes all the hydrogen absorbed during general corrosion is retained within the remaining drip shield wall thickness as the general corrosion process proceeds. It is most likely that the majority of it will be removed by conversion to the more thermodynamically stable titanium oxide as corrosion progresses. With the conservative assumption the hydrogen concentration in the drip shield increases continuously with time as the drip shield thickness (thus the volume of the remaining drip shield) is reduced by general corrosion. This hydrogen concentration increase from the thinning of the drip shield is in addition to the hydrogen pick-up from the general corrosion.

With the current conservative model, the time to have the hydrogen concentration in the drip shield exceed the critical hydrogen concentration could be before the time by general corrosion failure of the drip shield.

As noted in Section 6.1.3, crack growth in drip shield by HIC requires embrittlement of the drip shield (measured by the hydrogen concentration exceeding the critical hydrogen concentration) and applied stress. When the drip shield is subject to HIC, the failure will be by through-wall cracks, and the cracks are likely to be those generated by SCC. Those cracks are self-limited and will be eventually plugged by corrosion products and scale deposits (CRWMS M&O 2000c, Section 6.5.5). Therefore, even when the drip shield is breached by through-wall cracks induced by HIC, the intended design function of the drip shield (i.e., preventing dripping water from directly contacting the underlying waste package) will not be compromised significantly from the HIC failure.

### 6.2.5 Model Validation

Model validation has been accomplished following guidelines cited in ASTM procedure C 1174, 1997 (sections 19.3 and 20.4). According to ASTM C 1174 (section 20.4.3.1) validation of model means the model can account for all available data. In this AMR, data obtained in the laboratory for the Yucca Mountain Site Characterization Project along with published data available from the open scientific literature have been used to fit into well-known mathematical models to predict hydrogen induced corrosion behavior (e.g., corrosion rates, hydrogen concentration, etc.) of the proposed DS material (i.e., Ti-7). The model predicted values showed excellent agreement with the experimental data obtained by short-term laboratory tests. Additional data that are being collected will help improve the level of confidence in the model.

## 6.3 HYDROGEN INDUCED CRACKING OF TI-7 DUE TO GALVANIC COUPLE

### 6.3.1 Introduction

As indicated in Section 6.1.2, the three general conditions that must exist simultaneously for the hydrogen embrittlement of  $\alpha$  alloys are:

- A mechanism for generating hydrogen on a titanium surface.
- Metal temperature above approximately 80°C (175°F).
- Solution pH less than 3 or greater than 12, or impressed potentials more negative than -0.7 V(SCE).

In accordance with Schutz and Thomas (1987, p. 673), one hydrogen-generation mechanism is that coupling active metals such as zinc, magnesium, and aluminum can lead to hydrogen uptake and eventual embrittlement of titanium subjected to the temperature and other condition described above. A similar possible problem occurs when titanium is in galvanic contact with carbon steels. In a DS design without backfill, hydrogen generation may be caused by the galvanic couple between the titanium DS surface and structural components (such as rock bolts,

wire mesh, and steel liners used in the drift), which may fall onto the DS surface. Therefore, HIC or hydrogen embrittlement of the DS due to galvanic couple can not be ruled out since the conditions associated with metal temperature and water or moisture pH (or corrosion potential) as described above are certainly attainable under Yucca Mountain DS conditions.

### 6.3.2 Qualitative Assessment

Given the expected evolution of ground waters potentially contacting the drip shield and the temperature regime within the repository (CRWMS M&O 2000a, Section 1.3), the required conditions for hydrogen absorption by the titanium DS are clearly present when galvanically coupled to sections of the steel components. If occurring while temperatures are high ( $\geq 80^{\circ}\text{C}$ ) and concentrated ground waters are present, then local hydrided "hot spots" are possible. These "hot spots" will only occur at those sites where both contact to carbon steel and the establishment of lasting (at least periodically) aqueous conditions are achieved. Their formation is likely to be promoted if the contact points coincide with abraded or scratched areas of the shield caused by the impact of collapsing sections of the ground support structure.

At higher temperature, hydrogen will be more rapidly absorbed and transported into the bulk structure to produce the hydride distribution required for extensive crack propagation. It is less likely that a hydride layer will be retained at the surface. As the temperature falls, the formation of surface hydrides becomes more likely as the rate of hydrogen transport into the bulk of the metal decreases. The formation of surface hydrides tends to reduce the efficiency of subsequent hydrogen absorption (Noel et al. 1996), and their presence has little effect on structural integrity.

The efficiency of Fe-Ti galvanic couples to cause hydrogen cracking will be limited for a number of additional reasons:

1. The contact area is likely to be small, and the anode to cathode area (area of steel and titanium, respectively) low. Since relatively low volumes of groundwater are likely to contact both metals simultaneously, anode to cathode areas close to one seem likely. If a couple with a small anode to cathode area ratio was established (i.e., a small piece of steel in contact with a large area of drip shield), then one would expect the couple to be more rapidly exhausted as the steel is consumed. Under these conditions, the amount of hydrogen absorbed would be limited. Future quantitative studies may be conducted to determine: how much hydrogen would be liberated per unit mass of Fe; could that much hydrogen cause HIC in the adjacent Ti; and how fast does hydrogen diffuse into the surrounding Ti to keep hydrogen low?

While temperatures are high ( $>80^{\circ}\text{C}$ ), the intermittent nature of seepage dripping onto the drip shield should lead to only limited periods of the aqueous conditions required to sustain an active galvanic couple, thereby limiting hydrogen absorption while temperatures are high enough to drive hydrogen transport into the metal. For temperatures below  $80^{\circ}\text{C}$ , even galvanic polarization below the potential threshold of  $-0.6\text{ V}$  (vs SCE) produces only innocuous surface hydride films (Schutz and Thomas 1987). Also, at these lower temperatures, the small amounts of dissolved  $\text{O}_2$  in the solutions forming the galvanic couples will make it very difficult to achieve

polarization of the galvanic potential to less than -0.6 V (vs SCE). Additionally, the intermittent wetting and drying cycles anticipated on the drip shield will lead to the ready formation of calcareous and mineral deposits, which are well known to dramatically suppress galvanic currents, thereby stifling hydrogen absorption (Lunde and Nyborg 1993).

2. Conditions in the repository will be oxidizing, making it less likely that the couple will sustain water reduction, and hence hydrogen absorption. However, at high temperatures in concentrated saline solutions, the amount of O<sub>2</sub> dissolved in the solution forming the couple will probably be too low to displace water reduction as the primary cathodic reaction. However, the ferrous ion product of steel dissolution will be homogeneously oxidized to ferric species by dissolved O<sub>2</sub>. If conditions remain neutral, this should lead to the formation of insoluble Fe(III) oxides/hydroxides, and little influence would be exerted on the galvanic couple. However, any tendency for acidification or the development of alkaline conditions will increase the ferric ion solubility. Under evaporative conditions, this could lead to quite high dissolved ferric ion concentrations and the establishment of a galvanic potential sufficiently positive to avoid hydrogen absorption into the titanium. It is well documented that only parts per million concentrations of multivalent transition metal cations such as Fe(III) are required to polarize titanium to passive conditions (Schutz and Thomas 1987).
3. Titanium has a large tolerance for hydrogen (see Section 6.1.3 for critical hydrogen concentration), and substantial concentrations must be achieved before any degradation in fracture toughness is observed. This concentration level, as indicated in Section 6.1.3, has been measured to be in the range of 400 to 1000 μg.g<sup>-1</sup> for Ti-2 and Ti-12. Recent measurements suggest that the tolerance for hydrogen of the Ti-16 (a titanium alloy very similar to Ti-7 in chemical composition) may be in the 1000 to 2000 μg.g<sup>-1</sup> range (Ikeda and Quinn 1998, p. 7). According to Section 6.1.3, the critical hydrogen concentration for Ti-7 is 1000 μg.g<sup>-1</sup>.

Given the high critical hydrogen concentration, the large volume of available titanium in the drip shield into which absorbed hydrogen can diffuse, and other reasons stated above, hydrogen embrittlement of the Ti DS is highly unlikely.

### 6.3.3 Mathematical Model for Hydrogen Absorption and Diffusion in DS

As indicated in Section 6.3.2, hydrogen absorbed in the Ti-7 DS through the contact area of a galvanic couple may diffuse to the rest of the DS. A mathematical model is proposed in this section to predict the hydrogen concentration in the DS due to a galvanic couple between the DS and a carbon steel segment. The absorption and diffusion of hydrogen in the DS is a complex process. A mathematical model is possible only if a number of necessary assumptions are adopted. These assumptions are:

- The DS is treated as an infinite flat plate. The thickness of the plate is denoted as H.

- The contact plane between the DS surface and the carbon steel segment is circular in shape. The radius of the circular plane is denoted as  $r_0$ .
- Hydrogen is absorbed into the DS through the contact plane and immediately reaches the other surface. The initial region of the DS with hydrogen absorption has the shape of a circular disk with a radius  $r_0$  and thickness  $H$ .
- As hydrogen starts to diffuse in the DS, the radius of the circular region will expand at a constant speed  $v$ . As a result, the radius  $r(t)$  of the circular disk at a time  $t$  is expressed by the following equation:

$$r(t) = r_0 + v t \quad (\text{Eq. 4})$$

The amount of hydrogen (in g or mg, for example),  $Q(t)$ , absorbed in the DS at a time  $t$ , therefore, is:

$$Q(t) = \lambda(\rho_{\text{Ti}} \pi r_0^2) H t + \int_{\tau=0}^{\tau=t} \lambda \rho_{\text{Ti}} [2\pi r(\tau)] H (t - \tau) d\tau \quad (\text{Eq. 5})$$

where  $\lambda$  is the hydrogen absorption rate, in ppm (or  $\mu\text{g/g}$ ) /day, for example, and  $\rho_{\text{Ti}}$  is the mass density of the Ti-7 DS (see Section 6.1.5).

Based on the reaction:  $2\text{Fe} + 3\text{H}_2\text{O} \rightarrow \text{Fe}_2\text{O}_3 + 3\text{H}_2$ , the maximum amount of hydrogen that can be released from the carbon steel segment is:

$$Q_{\text{max}} = f_{\text{Fe}} 3W / M_{\text{Fe}} \quad (\text{Eq. 6})$$

where  $W$  is the mass of the carbon steel segment,  $f_{\text{Ti}}$  is the fraction of hydrogen produced by oxidation of the total mass of carbon steel, and  $M_{\text{Fe}}$  is the atomic mass of Fe.

If  $t_{\text{max}}$  is the time when  $Q(t)$  reaches  $Q_{\text{max}}$ ,  $t_{\text{max}}$  can be obtained by solving for the following equation:

$$Q_{\text{max}} = \lambda(\rho_{\text{Ti}} \pi r_0^2) H t_{\text{max}} + \int_{\tau=0}^{\tau=t_{\text{max}}} \lambda \rho_{\text{Ti}} [2\pi r(\tau)] H (t_{\text{max}} - \tau) d\tau \quad (\text{Eq. 7})$$

Using Eq. 4, Eq. 7 can be written as:

$$Q_{\text{max}} = \lambda \rho_{\text{Ti}} \pi H \left( r_0^2 t_{\text{max}} + r_0 v t_{\text{max}}^2 + \frac{v^2 t_{\text{max}}^3}{3} \right) \quad (\text{Eq. 8})$$

The maximum hydrogen concentration  $H_{\Lambda}(r_0)$  in ppm (or  $\mu\text{g/g}$ ), for example, will be in the region of the DS beneath the initial contact area and at the time  $t_{\text{max}}$ , i.e.,

$$H_A(r_0) = \lambda t_{\max} \quad (\text{Eq. 9})$$

The hydrogen concentration  $H_A(r)$  tends to reduce at location with a radius  $r$  from the center of the initial contact area, i.e.,

$$H_A(r) = \lambda \left( t_{\max} - \frac{r - r_0}{v} \right) \quad \text{for} \quad r_0 \leq r \leq r(t_{\max}) \quad (\text{Eq. 10})$$

At  $t > t_{\max}$ ,  $H_A(r)$  will start to decline as the hydrogen diffusion continues and the source of hydrogen exhausts.

As a numerical example, the following input data are considered:

$H$  = Ti-7 plate thickness = 15 mm

$r_0$  = radius of the initial contact area = 50.8 mm (2 in.)

$\rho_{\text{Ti}}$  = density of Ti-7 =  $4.5 \times 10^6$   $\mu\text{g}/\text{cm}^3$

$f_{\text{Fe}}$  = fraction of hydrogen available for absorption by Ti-7 DS = 0.01

$W$  = mass of carbon steel =  $22.727 \times 10^6$   $\mu\text{g}$  (50 lb.)

$M_{\text{Fe}}$  = atomic mass of Fe = 55.847 (Weast and Astle 1978, p. B-177)

The corrosion potential of carbon steel is estimated to be about -0.6 V (SCE), and a galvanic couple would polarize Ti down to that level. Based on Shoesmith et al. (1995, Figure 19) and Murai et al. (1977, Figure 5), the hydrogen absorption rate,  $\lambda$ , for Ti-7 would be about 0.5  $\mu\text{g}/\text{g}/\text{day}$ . No data are available for the hydrogen diffusion rate,  $v$ , in Ti-7. For the base case of the numerical example, the values used for  $\lambda$  and  $v$  are, respectively, 0.5  $\mu\text{g}/\text{g}/\text{day}$  and 1mm/day. For the parametric study,  $\lambda = 0.5, 0.7$   $\mu\text{g}/\text{g}/\text{day}$ , and  $v = 1, 2, 3$  mm/day are considered, and plots of hydrogen concentration versus distance from the original contact area are shown in Figure 2. It can be seen that, in all cases of the parametric study, the hydrogen concentration does not exceed the critical hydrogen concentration of 1000  $\mu\text{g}/\text{g}$  for Ti-7 by a rather comfortable margin. The results of the parametric study appear to be consistent with the qualitative assessment presented in Section 6.3.2. The choice of the mathematical model and the value of  $\lambda$  appear to be reasonable and conservative. The value of  $v$  is high, but would also appear to be reasonable, since it ignores the probability that the hydrogen will be retained at the Ti surface and that the efficiency of absorption would then decrease. The calculation can be considered bounding since all the features likely to suppress hydrogen absorption are ignored in the calculation. These features are summarized above in section 6.3.2.

### Hydrogen Concentration in Drip Shield due to Galvanic Couple

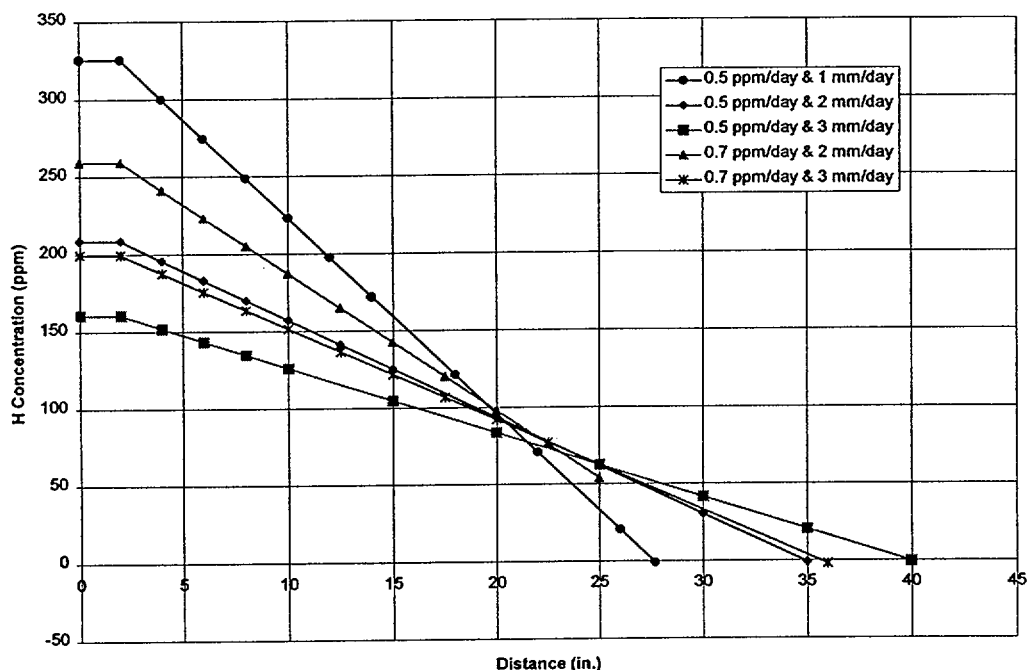


Figure 2. Hydrogen Concentration in Drip Shield Versus Distance from Contact Area

#### 6.3.4 Worst Case Considerations

As a worst case scenario, it is considered that the majority portion of the hydrogen generated by the section of carbon steel will be absorbed by the DS, and that the absorbed hydrogen will be retained in the vicinity of the contact area and not to be diffused to the rest of the DS. In this case, there may be a local embrittlement of the DS in the contact area. It is further considered that the contact area is impacted by a rock fall, and residual stress and a crack are initiated. As a result, a fast brittle fracture is possible if the stress intensity factor calculated from the residual stress and the crack size exceeds the fast fracture stress intensity factor  $K_{IH}$ , which tends to have a reduced value than the critical slow crack growth stress intensity factor  $K_{IS}$  (also called fracture toughness) as indicated in Figure 1.

Calculated stress intensity factors due to rock fall in the DS are listed in CRWMS M&O (2000c, Attachment II) for various crack sizes (depths). Based on CRWMS M&O (2000c), an initial crack depth of  $50\mu\text{m}$  (i.e., the maximum incipient crack size, based on CRWMS M&O 2000c, Section 6.5.2) can be assumed. The equivalent stress intensity factor, based on CRWMS M&O (2000c, Attachment II), is  $< 5 \text{ MPa (m)}^{0.5}$ . From CRWMS M&O (2000c, Figure 27), it can be seen that the fracture toughness  $K_{IS}$  for Ti-7 should be at least  $30 \text{ MPa (m)}^{0.5}$ . Assuming  $K_{IH} = 1/3 K_{IS} = 10 \text{ MPa (m)}$ , brittle fracture due to hydrogen embrittlement would not be a problem for the DS subjected to a galvanic couple with a section of carbon steel structural component.

Even though fast brittle fracture does occur and the surface crack turns into a through-wall crack, the length of the crack will still be limited because the surrounding area of the DS is not

embrittled by hydrogen. The crack opening will eventually be plugged by corrosion product (CRWMS M&O 2000c, Section 6.5.5).

## 7. CONCLUSIONS

A simple and conservative model has been developed to evaluate the effects of hydrogen induced cracking on the drip shield. The basic premise of the model is that failure will occur once the hydrogen content exceeds a certain limit or critical value,  $H_c$ . Quantitative evaluation based on the HIC model described in Section 6.1 indicates that the drip shield material (Ti-7) is able to sustain the effects of HIC.

The quantitative evaluation includes analytical estimates presented in Section 6.2.3 based on Equation 2, indicating that there exists a big margin of safety for the drip shield against the effects of HIC. The hydrogen concentration in the DS at 10,000 years after emplacement is 257  $\mu\text{g/g}$  resulting from a conservative estimate and 58  $\mu\text{g/g}$  from a best estimate. The estimated hydrogen concentration in either case is less than the critical hydrogen concentration of 1000  $\mu\text{g/g}$  for Ti-7, a conservative value based on Section 6.1.3.

Model validation in this AMR was accomplished using short term data available to date. Additional data that are being collected will help improve the level of confidence in the model.

In a DS design without backfill, hydrogen generation may be caused by the galvanic couple between the titanium DS surface and structural components (such as rock bolts, wire mesh, and steel liners used in the drift), which may fall onto the DS surface. A qualitative assessment of HIC due to effects of galvanic couple, as presented in Section 6.3.2, concludes that, given the high critical hydrogen concentration, the large volume of available titanium in the drip shield into which absorbed hydrogen can diffuse, and other reasons stated in Section 6.3, hydrogen embrittlement of the Ti DS is highly unlikely.

A parametric study based on a proposed mathematical model (Section 6.3.3) indicates that hydrogen concentration in the DS due to a galvanic couple will most likely not exceed the critical value. Consideration of the worst case scenario leads to the conclusion that hydrogen embrittlement is unlikely even though the hydrogen concentration may exceed the critical value because the stress intensity factor induced by a rock fall appears to be below the fracture toughness which although may be degraded by hydrogen content. Furthermore, if cracks do become through wall, they will be self-limited and eventually plugged by corrosion product.

This document may be affected by technical product input information that requires confirmation. Any changes to the document that may occur as a result of completing the confirmation activities will be reflected in subsequent revisions. The status of the input information quality may be confirmed by review of the Document Input Reference System database.

## 8. INPUTS AND REFERENCES

### 8.1 DOCUMENTS CITED

ASM International 1987. *Corrosion*. Volume 13 of *Metals Handbook*. 9th Edition. Metals Park, Ohio: ASM International. TIC: 209807.

Beck, T.R. 1973. "Electrochemistry of Freshly-Generated Titanium Surfaces - I. Scraped-Rotating-Disk Experiments." *Electrochimica Acta*, 18, 807-814. [New York, New York]: Pergamon Press. TIC: 248519.

Clarke, C.F.; Hardie, D.; and Ikeda, B.M. 1995. *Hydrogen Induced Cracking of Grade-2 Titanium*. AECL-11284. Pinawa, Manitoba, Canada: Whiteshell Laboratories. TIC: 226150.

CRWMS M&O 1999a. *Classification of the MGR Uncanistered Spent Nuclear Fuel Disposal Container System*. ANL-UDC-SE-000001 REV 00. Las Vegas, Nevada: CRWMS M&O. ACC: MOL.19990928.0216.

CRWMS M&O 1999b. Not used.

CRWMS M&O 1999c. Not used.

CRWMS M&O 1999d. *Waste Package Material Properties*. BBA000000-01717-0210-00017 REV 00. Las Vegas, Nevada: CRWMS M&O. ACC: MOL.19990407.0172.

CRWMS M&O 1999e. *1101213PM7 Waste Package Analyses & Models - PMR*. Activity Evaluation, September 21, 1999. Las Vegas, Nevada: CRWMS M&O. ACC: MOL.19991012.0219.

CRWMS M&O 1999f. *Analysis and Model Reports to Support Waste Package PMR*. TDP-EBS-MD-000003 REV 00. Las Vegas, Nevada: CRWMS M&O. ACC: MOL.19990809.0401.

CRWMS M&O 2000a. *General Corrosion and Localized Corrosion of the Drip Shield*. ANL-EBS-MD-000004 REV 00. Las Vegas, Nevada: CRWMS M&O. ACC: MOL.20000329.1185.

CRWMS M&O 2000b. *Emplacement Drift System Description Document*. SDD-EDS-SE-000001 REV 01. Las Vegas, Nevada: CRWMS M&O. ACC: MOL.20000803.0348.

CRWMS M&O 2000c. *Stress Corrosion Cracking of the Drip Shield, the Waste Package Outer Barrier and the Stainless Steel Structural Material*. ANL-EBS-MD-000005 REV 00 ICN 01. Las Vegas, Nevada: CRWMS M&O. URN-0588

DOE (U.S. Department of Energy) 2000. *Quality Assurance Requirements and Description*. DOE/RW-0333P, Rev. 10. Washington, D.C.: U.S. Department of Energy, Office of Civilian Radioactive Waste Management. ACC: MOL.20000427.0422.

Harrar, J.E.; Carley, J.F.; Isherwood, W.F.; and Raber, E. 1990. *Report of the Committee to Review the Use of J-13 Well Water in Nevada Nuclear Waste Storage Investigations*. UCID-21867. Livermore, California: Lawrence Livermore National Laboratory. ACC: NNA.19910131.0274.

Ikeda, B.M. and Quinn, M.J. 1998. *Hydrogen Assisted Cracking of Grade-16 Titanium: A Preliminary Examination of Behavior at Room Temperature*. 06819-REP-01200-0039 R00. 13. Toronto, Ontario, Canada: Ontario Hydro. TIC: 247312.

Lunde, L. and Nyborg, R. 1993. *Hydrogen Absorption of Titanium Alloys During Cathodic Polarization*. Paper No. 5. Houston, Texas: [National Association of Corrosion Engineers]. TIC: 248523.

Murai T.; Ishikawa, M.; and Miura, C. 1977. "The Absorption of Hydrogen into Titanium Under Cathodic Polarization." *Corrosion Engineering*, 26, (4), 177-183. [Tokyo, Japan]: Japan Society of Corrosion Engineering. TIC: 246349.

Noel, J.J.; Bailey, M.G.; Crosthwaite, J.P.; Ikeda, B.M.; Ryan, S.R.; and Shoesmith, D.W. 1996. *Hydrogen Absorption by Grade-2 Titanium*. AECL-11608. Pinawa, Manitoba, Canada: Atomic Energy of Canada Limited, Whiteshell Laboratories. TIC: 246232.

NRC (U.S. Nuclear Regulatory Commission) 1999. *Issue Resolution Status Report Key Technical Issue: Container Life and Source Term*. Rev. 2. Washington, D.C.: U.S. Nuclear Regulatory Commission. TIC: 245538.

Okada, T. 1983. "Factors Influencing the Cathodic Charging Efficiency of Hydrogen by Modified Titanium Electrodes." *Electrochimica Acta*, 28, (8), 1113-1120. New York, New York: Pergamon Press. TIC: 246262.

Schutz, R.W. 1988. "Titanium Alloy Crevice Corrosion: Influencing Factors and Methods of Prevention." *Proceedings of the Sixth World Conference on Titanium, Cannes, June 6-9, 1988*. Lacombe, P.; Tricot, R.; and Beranger, G., eds. IV, 1917-1922. Cedex, France: Societe Francaise de Metallurgie. TIC: 248782.

Schutz, R.W. and Thomas, D.E. 1987. "Corrosion of Titanium and Titanium Alloys." Volume 13 of *Metals Handbook*. 9th Edition. Pages 669-706. Metals Park, Ohio: ASM International. TIC: 209807.

Shoesmith, D.W.; Hardie, D.; Ikeda, B.M.; and Noel, J.J. 1997. *Hydrogen Absorption and the Lifetime Performance of Titanium Waste Containers*. AECL-11770. Pinawa, Manitoba, Canada: Atomic Energy of Canada Limited. TIC: 236220.

Shoesmith, D.W.; Ikeda, B.M.; Bailey, M.G.; Quinn, M.J.; and LeNeveu, D.M. 1995. *A Model for Predicting the Lifetimes of Grade-2 Titanium Nuclear Waste Containers*. AECL-10973. Pinawa, Manitoba, Canada: Atomic Energy of Canada Limited. TIC: 226419.

Weast, R.C. and Astle, M.J., eds. 1978. *CRC Handbook of Chemistry and Physics*. 59th Edition. pp. D-265, D-299, D-300, D-304, F-61 and F-62. Boca Raton, Florida: CRC Press. TIC: 246395.

## 8.2 CODES, STANDARDS, REGULATIONS, AND PROCEDURES

AP-2.21Q, Rev. 0, ICN 0. *Quality Determinations and Planning for Scientific, Engineering, and Regulatory Compliance Activities*. Washington, D.C.: U.S. Department of Energy, Office of Civilian Radioactive Waste Management. ACC: MOL.20000802.0003.

ASTM C 1174-97. 1997. *Standard Practice for Prediction of the Long-Term Behavior of Materials, Including Waste Forms, Used in Engineered Barrier Systems (EBS) for Geological Disposal of High-Level Radioactive Waste*. West Conshohocken, Pennsylvania: American Society for Testing and Materials. TIC: 246015.

QAP-2-3, Rev. 10. *Classification of Permanent Items*. Las Vegas, Nevada: CRWMS M&O. ACC: MOL.19990316.0006.

QAP-2-0, Rev. 5. *Conduct of Activities*. Las Vegas, Nevada: CRWMS M&O. ACC: MOL.19980826.0209.